Supplementary Materials

Table S1. Statistics of morphological parameters characterizing street changes based on opening effective points for street cases.

Street ID	N_OEP	Location of OEP [m]	L_OEP [m]
A1	4	82, 134, 163, 217	4, 13, 37, 23
A2	3	77, 189, 253	6, 31, 24
A3	7	72, 132, 185, 229, 291, 349, 376	5, 22, 31, 19, 33, 22, 11
A4	5	64, 168, 249, 276, 290	22, 43, 23, 14, 6
A5	1	173	28
A6	3	111, 237, 327	6, 119, 9
A7	7	65, 92, 120, 185, 236, 326, 399	5, 21, 9, 20, 6, 14, 10
A8	4	124, 179, 261, 304	10, 69, 8, 16
B1	4	108, 155, 168, 188	14, 5, 11, 6
B2	3	56, 116, 206	12, 11, 8
B3	1	73	15
B4	0	/	/
B5	1	113	19
C1	6	27, 71, 85, 103, 125, 149	11, 9, 9, 12, 14, 12
C2	5	113, 160, 175, 189, 252	21, 6, 12, 10, 14
C3	12	28, 52, 71, 103, 128, 154, 177, 191, 213, 234, 253, 269	6, 7, 18, 26, 18, 27, 6, 8, 9, 14, 9, 6
C4	0	/	/
C5	2	39, 60	7, 5
C6	0	/	/
C7	1	77	8

Table S2. Statistics of morphological parameters characterizing street changes based on building effective points for street cases.

Street ID	N_BEP	Location of BEP [m]	AR of BEP	BHR of BEP
A1	22	34, 46, 59, 69, 76, 86, 103, 121, 182, 189, 234, 247, 254, 259, 292, 327, 332, 338, 346, 359, 366, 371	0.18, 0.22, 0.26, 0.27, 0.32, 0.18, 0.18, 0.16, 0.13, 0.13, 0.13, 0.19, 0.19, 0.37, 0.42, 0.29, 0.29, 0.25, 0.23, 0.08, 0.08, 0.07	1, 1, 1, 1.17, 1, 0.43, 0.5, 0.5, 1.8, 1.8, 1.5, 2.25, 2.25, 1.125, 1, 0.21, 0.21, 0.19, 0.19, 2, 2, 2.25
A2	14	60, 68, 84, 93, 109, 136, 151, 159, 219, 237, 285, 331, 351, 363	0.08, 0.08, 0.14, 0.18, 0.2, 0.37, 0.37, 0.10, 0.29, 0.31, 0.18, 0.42	0.6, 0.6, 2.4, 2.1, 2.1, 1.3, 1.3, 2.4, 5.5, 3.3, 1.8, 1.8, 3.3, 1.4
A3	24	41, 54, 64, 76, 89, 103, 112, 119, 147, 158, 164, 202, 209, 216, 243, 252, 261, 270, 312, 324, 334, 365, 392, 422	0.18, 0.21, 0.16, 0.03, 0.23, 0.04, 0.18, 0.21, 0.32, 0.31, 0.27, 0.20, 0.21, 0.13, 0.21, 0.21, 0.21, 0.21, 0.38, 0.43, 0.21, 0.39, 0.36, 0.35	1.4, 2.0, 0.8, 0.3, 2.0, 0.3, 2.0, 2.0, 1.3, 1.3, 1.3, 0.6, 0.6, 0.6, 0.4, 0.3, 0.3, 0.3, 1.0, 1.0, 1.0, 1.0, 0.8, 1.0
A4	10	38, 82, 96, 111, 131, 211, 265, 285, 297, 307	0.04, 0.27, 0.22, 0.14, 0.25, 0.24, 0.02, 0.16, 0.18, 0.18	8.0, 0.8, 1.3, 0.4, 0.7, 0.3, 6.0, 1.0, 2.5, 2.5

A5	13	47, 68, 84, 110, 135, 143, 153, 190, 214, 246, 260, 268, 281	0.14, 0.17, 0.06, 0.37, 0.22, 0.19, 0.16, 0.21, 0.24, 0.26, 0.13, 0.24, 0.21	2.0, 6.0, 6.0, 1.1, 1.6, 1.6, 1.6, 0.8, 0.8, 0.8, 1.3, 0.6, 0.6
A6	11	54, 63, 72, 77, 97, 134, 162, 171, 298, 311, 339, 339	0.17, 0.30, 0.35, 0.23, 0.23, 0.41, 0.22, 0.19, 0.15, 0.08, 0.08	0.5, 0.7, 0.7, 0.4, 0.6, 3.3, 0.6, 0.6, 0.3, 0.2, 0.2
A7	21	60, 71, 78, 107, 133, 143, 152, 165, 173, 204, 223, 248, 263, 289, 315, 338, 355, 380, 391, 425, 448	0.34, 0.14, 0.10, 0.11, 0.07, 0.14, 0.15, 0.14, 0.07, 0.06, 0.17, 0.17, 0.09, 0.17, 0.19, 0.14, 0.14, 0.10, 0.25, 0.05, 0.06	1.3, 4.0, 4.0, 1.3, 0.5, 1.0, 0.7, 0.7, 2.0, 6.0, 2.0, 2.0, 3.0, 1.2, 5.0, 0.2, 0.3, 0.3, 3.3, 0.1, 0.5
A8	11	83, 102, 136, 217, 240, 268, 276, 282, 290, 314, 340	0.04, 0.43, 0.30, 0.03, 0.06, 0.04, 0.05, 0.08, 0.04, 0.16, 0.16	0.1, 0.5, 0.4, 20.0, 10.0, 0.3, 0.3, 0.6, 3.3, 0.8, 0.6
B1	11	36, 45, 72, 96, 121, 138, 159, 179, 210, 236, 242	0.49, 0.62, 0.73, 0.25, 0.69, 0.79, 0.80, 0.83, 0.12, 0.23, 0.13	0.9, 0.9, 0.9, 0.3, 0.9, 0.9, 0.9, 0.8, 0.1, 0.3, 1.0
B2	14	4, 38, 53, 72, 78, 95, 99, 114, 129, 137, 156, 189, 199, 222	0.27, 0.23, 0.31, 0.38, 0.46, 0.41, 0.35, 0.69, 0.11, 0.39, 0.46, 0.18, 0.33, 0.38	0.3, 0.4, 0.3, 0.6, 0.4, 0.3, 0.5, 0.5, 0.1, 0.4, 0.4, 1.5, 0.4, 0.5
B3	4	45, 83, 97, 112	0.39, 0.27, 0.36, 0.29	1.5, 8.3, 8.3, 8.3
B4	8	23, 29, 37, 51, 66, 79, 91, 107	2.0, 2.0, 2.0, 1.6, 1.3, 1.3, 1.3, 1.3	0.41, 0.42, 0.46, 0.45, 0.67, 0.88, 0.76, 0.67
B5	9	44, 53, 59, 68, 88, 128, 159, 188, 196	0.21, 0.23, 0.27, 0.30, 0.49, 1.14, 0.69, 0.69, 0.58	0.5, 0.5, 0.5, 0.5, 0.5, 4.2, 0.5, 0.8, 0.5
C1	9	15, 40, 56, 77, 91, 112, 137, 161, 169	0.38, 0.21, 0.20, 0.35, 0.18, 0.87, 1.07, 1.15, 0.29	3.0, 0.2, 0.1, 3.0, 0.3, 1.0, 1.3, 1.0, 4.0
C2	16	80, 94, 99, 128, 141, 151, 155, 166, 183, 199, 205, 215, 235, 244, 263, 268	0.14, 0.17, 0.18, 0.15, 0.15, 0.19, 0.98, 0.53, 0.48, 0.35, 0.35, 0.35, 0.63, 0.32, 0.22, 0.42	0.1, 0.2, 0.2, 0.2, 0.0, 0.2, 1.0, 0.6, 3.0, 6.0, 1.0, 0.5, 3.0, 0.5, 2.0, 0.7
C3	15	15, 22, 40, 58, 85, 117, 139, 170, 184, 201, 222, 245, 261, 277, 283	0.33, 0.33, 0.26, 0.52, 1.03, 0.21, 1.17, 1.06, 0.48, 1.46, 0.93, 0.94, 0.88, 0.33, 0.32	1.0, 0.3, 3.3, 1.7, 0.6, 0.2, 1.8, 1.8, 0.6, 1.0, 1.0, 0.6, 1.0, 3.3, 1.0
C4	4	64, 82, 104, 113	0.24, 0.20, 0.32, 0.52	0.3, 0.3, 0.5, 0.8
C5	5	33, 48, 62, 76, 85	0.66, 0.42, 0.45, 0.32, 0.67	1.8, 3.0, 3.0, 6.0, 3.0
C6	4	37, 55, 81, 97	0.39, 0.52, 0.94, 0.93	0.6, 0.2, 0.3, 1.0
C7	4	10, 39, 67, 105	0.67, 0.66, 0.66, 1.43	1.0, 1.0, 1.0, 1.0

Note S1. Wind tunnel measurements, CFD modelling and validation.

The specific wind tunnel measurements, CFD modelling, and validation are described below.

S1. Wind Tunnel Measurements

The accuracy of the simulation model is verified by wind tunnel tests [1]. The experiments were conducted at the atmospheric boundary layer wind tunnel in the State

Environmental Protection Key Laboratory of Atmospheric Physical Modelling and Pollution Control, China. The closed-circuit wind tunnel was 24 m long, with a section size of 4 m wide and 3 m high. A simple 1:400 scale model of the Xinjiekou area was placed on a 3.6-meter diameter turntable (Figure S1). The blockage ratio was 4.75%, which met the standard requirement for the wind tunnel tests of buildings and structures JGJ/T 338–2014 [2]. The average wind speed was measured using hot-wire anemometers at 50 selected points at the 0.005 m level (2 m for full-scale).

Figure S1. The model image in the wind tunnel.

S2. CFD Modelling

S2.1. CFD Approach and Model Set-Up

A computational fluid dynamics (CFD) approach was used to simulate the wind field at pedestrian level (height = 2 m) in the study area. This study used the Reynolds-Averaged Navier–Stokes (RANS) equations with a k-ε turbulence model to solve for the turbulent airflow parameters in the computational domain. RANS equations with a realizable k-ε turbulence model are widely used in the simulation of urban ventilation with high accuracy when the wind flow prediction is focused on the average wind speed [3]. The CFD model set-up followed the main simulation requirements that were provided by the guidelines of the Architectural Institute of Japan guidelines and the European Cooperation in Science and Technology action [4, 5]. The computational domain of the buildings has the same cross-section as the wind tunnel in the lateral directions. The height of the domain was 11 Hmax, where Hmax was the maximum building height, while the upstream and downwind domain sizes were 5 Hmax and 15 Hmax, respectively (Figure S2). The model set-up also used a reduced-scale 1:400 of building size, which is in line with the wind tunnel test. The computational domain was constructed with tetrahedral cells, where each side of the buildings or streets had at least ten cells. Four cells were included at pedestrian level along the vertical direction, with an expansion ratio of less than 1.2. By comparing the wind speed ratios at different locations on coarse, medium and fine grids, it was found that the effect of the error caused by the change in grid resolution on the numerical results was negligible, and the medium grid resolution was chosen for this study. The SIMPLE Method for the pressure-linked equations algorithm was utilised for pressure–velocity coupling. The pressure interpolation, the convection, and the viscous terms of the governing equations exhibited second-order accuracy. The simulations were performed until the residuals remained constant. Overall, in terms of the residual for the continuity equation, the velocity components, k and ε, were equal to or < 10−5. The ANSYS-Fluent software was used as the calculation tool, which is a commonly adopted CFD simulation software.

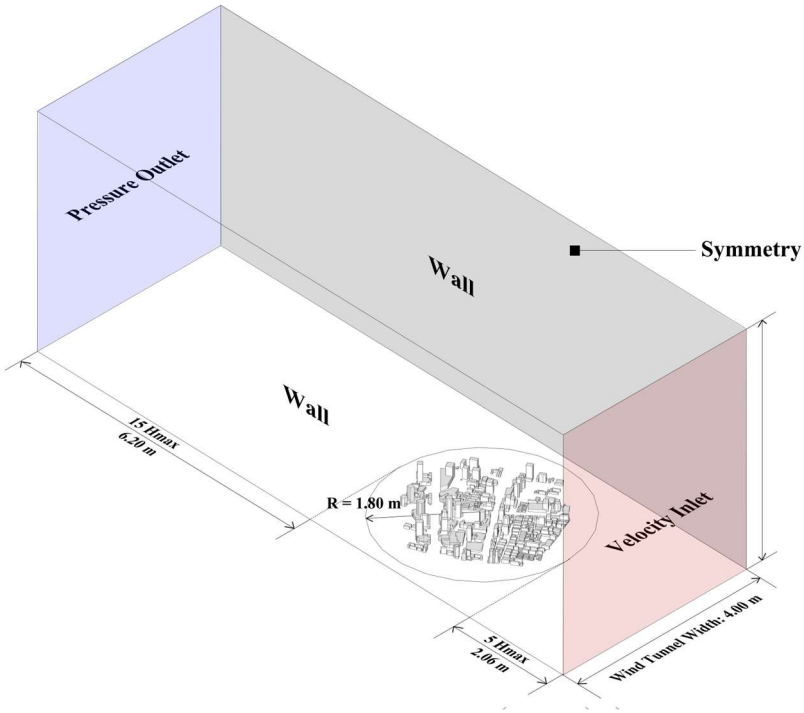

Figure S2. Calculation domain and boundary conditions in computational fluid dynamics (CFD) simulation.

S2.2. CFD Model Validation

To validate the accuracy of the CFD results, fifty measurement points were randomly selected in the study area and their CFD simulation results were compared with the wind tunnel test results. The root mean square error (RMSE) of the wind speed ratio between the CFD simulation and the wind tunnel test was 0.02, which is close to the RMSE value of 0.08 ~ 0.24 found in similar validation studies, indicating the credibility of the CFD results [6]. More than 80% of the CFD simulations were generally within 20% of the measurement error. This result was close to the research conducted by Blocken, Stathopoulos, and van Beeck's research, which demonstrated that steady RANS modelling generates accurate results (between 10-20%) [7].

References for Note S1

1. Li, J.; You, W.; Ding, W. Exploring Urban Space Quantitative Indicators Associated with Outdoor Ventilation Potential. *Sustainable Cities and Society* **2022**, *79*, 103696, doi:10.1016/j.scs.2022.103696.
2. Jin, X. Y.; Chen, K.; Jin, H.; Li, Q. X.; Cao, S. Y.; Quan, Y.; Li, S. Y.; Li, M. S.; Lou, W. J.; Liu, J. X.; et al. *Standard for Wind Tunnel Test of Buildings and Structures (JGJ/T338-2014)*; China Architecture & Building Press: Beijing, China, 2014. (in Chinese).
3. Lin, M.; Hang, J.; Li, Y.; Luo, Z.; Sandberg, M. Quantitative Ventilation Assessments of Idealized Urban Canopy Layers with Various Urban Layouts and the Same Building Packing Density. *Building and Environment* **2014**, *79*, 152–167, doi:10.1016/j.buildenv.2014.05.008.
4. Franke, J.; Hellsten, A.; Schlunzen, K.H.; Carissimo, B. The COST 732 Best Practice Guideline for CFD Simulation of Flows in the Urban Environment: A Summary. *IJEP* **2011**, *44*, 419, doi:10.1504/IJEP.2011.038443.
5. Tominaga, Y.; Mochida, A.; Yoshie, R.; Kataoka, H.; Nozu, T.; Yoshikawa, M.; Shirasawa, T. AIJ Guidelines for Practical Applications of CFD to Pedestrian Wind Environment around Buildings. *Journal of Wind Engineering and Industrial Aerodynamics* **2008**, *96*, 1749–1761, doi:10.1016/j.jweia.2008.02.058.
6. Mo, Z.; Liu, C.-H.; Ho, Y.-K. Roughness Sublayer Flows over Real Urban Morphology: A Wind Tunnel Study. *Building and Environment* **2021**, *188*, 107463, doi:10.1016/j.buildenv.2020.107463.
7. Blocken, B. LES over RANS in Building Simulation for Outdoor and Indoor Applications: A Foregone Conclusion? *Build. Simul.* **2018**, *11*, 821–870, doi:10.1007/s12273-018-0459-3.